II. MICROWAVE GASEOUS DISCHARGES*

Prof. S. C. Brown
Prof. W. P. Allis
Prof. D. J. Rose
Prof. D. R. Whitehouse
Dr. G. Bekefi
Dr. L. Mower
C. D. Buntschuh
J. D. Coccoli
S. Frankenthal
R. B. Hall
R. L. Hall
J. L. Hirshfield
W. R. Kittredge
J. J. McCarthy
W. J. Mulligan
G. B. Nichols
J. J. Nolan, Jr.
Judith S. Vaughen
C. S. Ward

A. NORMAL WAVE SURFACES FOR ELECTROMAGNETIC WAVES IN A PLASMA

Many papers that consider the effects of terminal motions, finite Larmor radius, collisions, and so forth on the propagation of plane waves through a plasma in the presence of a magnetic field have recently appeared (1, 2, 3, 4). The necessary mathematics obscures the origin of many of the predicted phenomena, and as these also depend critically on the range of frequency, plasma density, and the magnetic field that is considered, it has seemed worth while to view the complete range of these last three variables in the simple limit in which there are: (a) no density gradients; (b) no collisions; and (c) no thermal motions. The thermal motions affect mainly the slow waves whose phase velocity is comparable to the thermal motions. For this reason, among others, we shall be particularly interested to note the conditions under which slow waves exist.

Under these restrictions, the mobility of an electron or ion in a magnetic field is a tensor quantity (5) that is particularly simple when it is expressed in components of the electric field which are either parallel (μ_p) or rotating about the magnetic field in a right-handed (μ_r) or left-handed (μ_ℓ) direction. In terms of the mobility tensor, we obtain the plasma conductivity,

$$\overleftrightarrow{\sigma} = \Sigma\, nq\, \overleftrightarrow{\mu}_{\pm} \tag{1}$$

by summing over the species of charged particles, and hence the effective dielectric coefficient

$$\overleftrightarrow{K} = \begin{vmatrix} K_T & jK_H & 0 \\ -jK_H & K_T & 0 \\ 0 & 0 & K_p \end{vmatrix} = 1 + \frac{\overleftrightarrow{\sigma}}{j\omega\epsilon_o} \tag{2}$$

where

$$\begin{aligned} 2K_T &= K_r + K_\ell \\ 2K_H &= K_r - K_\ell \end{aligned} \tag{3}$$

---

*This work was supported in part by the Atomic Energy Commission under Contract AT(30-1)1842.

The tensor (Eq. 2) is written in Cartesian, nonrotating coordinates. K_p and K_T are the components parallel and transverse to the magnetic field, and K_H is the component that gives the Hall effect. The last two components are given in terms of the rotating components by Eqs. 3.

For the particular case of a collisionless, cold, three-component (ions, electrons, and neutral molecules) gas the components of the dielectric tensor are

$$\left.\begin{aligned} K_p &= 1 - a^2 \\ K_r &= 1 - a^2/(1 + \beta_+)(1 - \beta_-) \\ K_\ell &= 1 - a^2/(1 - \beta_+)(1 + \beta_-) \end{aligned}\right\} \tag{4}$$

They are expressed simply in terms of the ratios

$$\left.\begin{aligned} a^2 &= \frac{\omega_p^2}{\omega^2} = \frac{ne^2(m_+ + m_-)}{\epsilon_o m_+ m_- \omega^2} \\ \beta_\pm &= \frac{\omega_{b\pm}}{\omega} = \frac{eB}{m_\pm \omega} \end{aligned}\right\} \tag{5}$$

where a^2 is a measure of the plasma density n, $\beta_\pm$ of the applied magnetic field B, and a, β_+, β_- all vary inversely with the circular frequency ω of the electric field.

We now study plane waves by assuming that all quantities are proportional to

$$\exp j\omega(t - \vec{n} \cdot \vec{r}/c) \tag{6}$$

where $\vec{n}$ is a vector normal to the wave whose magnitude n is the index of refraction for this direction of propagation. There should be no confusion in the use of the same letter in formula 5 because the plasma density will only appear implicitly in the symbol a. The phase velocity is

$$\vec{u} = \frac{c\vec{n}}{n^2} \tag{7}$$

Substituting expression 6 in Maxwell's equations, we obtain

$$\vec{n} \times (\vec{n} \times \vec{E}) + \overleftrightarrow{K} \cdot \vec{E} = 0 \tag{8}$$

This equation, among others, has been considered by Aström (6). To obtain solutions, the determinant of its coefficients must vanish, and this gives the dispersion equation for the index of refraction n. This equation would, in general, be bi-cubic but, because the temperature has been neglected, the sixth degree terms cancel and we have the

bi-quadratic equation

$$An^4 - Bn^2 + C = 0 \tag{9}$$

with

$$A = K_T \sin^2 \theta + K_p \cos^2 \theta$$

$$B = K_r K_\ell \sin^2 \theta + K_p K_T (1 + \cos^2 \theta)$$

$$C = K_p K_r K_\ell$$

whose discriminant is

$$D^2 = 4K_p^2 K_H^2 \sin^2 \theta + (K_r K_\ell - K_p K_T)^2 \cos^4 \theta \tag{10}$$

Here θ is the angle between the wave normal $\vec{n}$ and the applied magnetic field $\vec{B}$.

Because collisions have been neglected, the discriminant D^2 is always positive. Therefore, n^2 is always real, and n either real or pure imaginary. This sharp distinction between conditions of propagation or attenuation exists in virtue of assumptions (a), (b), and (c).

The solutions of Eq. 9 are the indices of refraction

$$n = \left(\frac{(B \pm D)}{2A} \right)^{1/2} \tag{11}$$

associated with the two polarizations, but it is easier to understand the solutions of Eq. 9 if it is solved for the direction of propagation, θ, in terms of the index n:

$$\tan^2 \theta = - \frac{K_p \left(n^2 - K_r \right) \left(n^2 - K_\ell \right)}{\left(n^2 - K_p \right) \left(K_T n^2 - K_r K_\ell \right)} \tag{12}$$

In this form it is clear that for propagation along the magnetic field (θ=0) there are two waves

$$n_r^2 = K_r$$

$$n_\ell^2 = K_\ell \tag{13}$$

that may be either propagated or attenuated according to the signs of K_r and K_ℓ, and the subscripts on the dielectric components indicate that they are right and left circularly polarized.

Similarly, for propagation at right angles across the magnetic field ($\theta = \pi/2$) there are two waves

$$n_o^2 = K_p$$
$$n_x^2 = K_r K_\ell / K_T \tag{14}$$

of which the first is polarized with the electric field parallel to the applied magnetic field. We shall call this wave "ordinary" because it is not affected by the magnetic field. The second wave, which we shall call "extraordinary," is transverse to the magnetic field but not transverse to the direction of propagation. It is made up of electric vectors rotating right- and left-handed around B, describing an ellipse in a plane perpendicular to B which contains the direction of propagation. Thus

$$\frac{2}{n_x^2} = \frac{1}{n_r^2} + \frac{1}{n_\ell^2} \tag{15}$$

The extraordinary velocity is intermediate between the right- and left-handed velocities.

For intermediate directions ($0 < \theta < \pi/2$) the index is intermediate between the "principal indexes" given by Eqs. 13 and 14. If we make a polar plot of the phase velocity $\vec{u}$, we obtain two surfaces, called "normal wave surfaces," like those shown in Figs. II-1, II-2, and II-3. Since D is never zero, the two wave surfaces do not intersect.

In crystal optics the term "ordinary" is used for waves that obey Snell's law, that is, those for which the wave surface is spherical. In our case neither surface is spherical except in limiting situations. The term "ordinary" does not apply to either

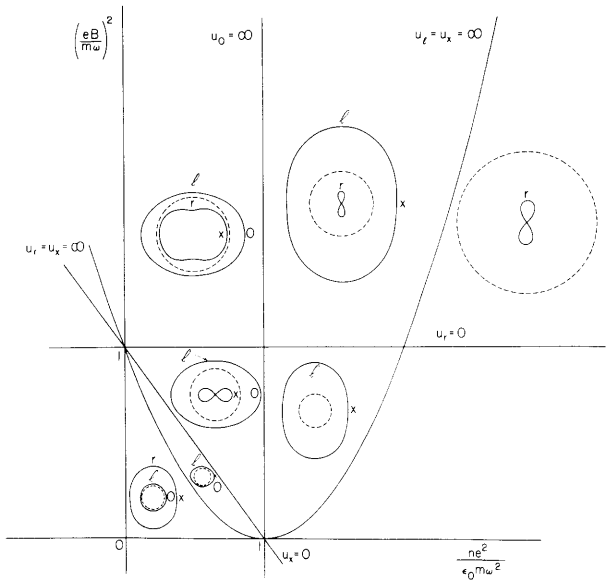

Fig. II-1. Wave normal surfaces of a plasma in a magnetic field. (Effect of electrons only.)

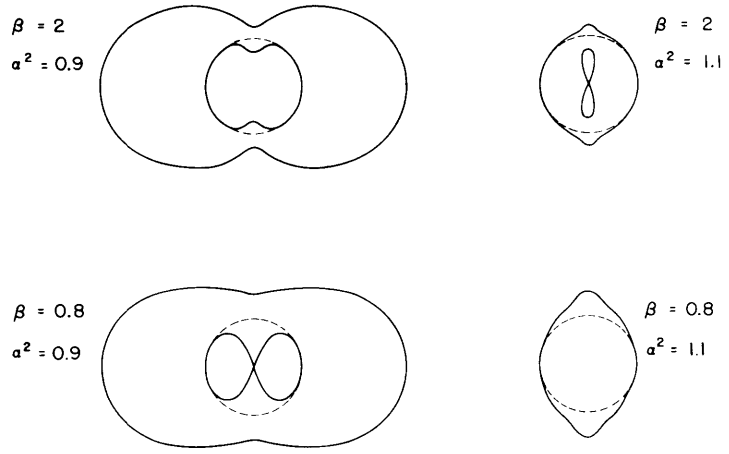

Fig. II-2. Wave normal surfaces in the vicinity of $\alpha^2 = 1$.

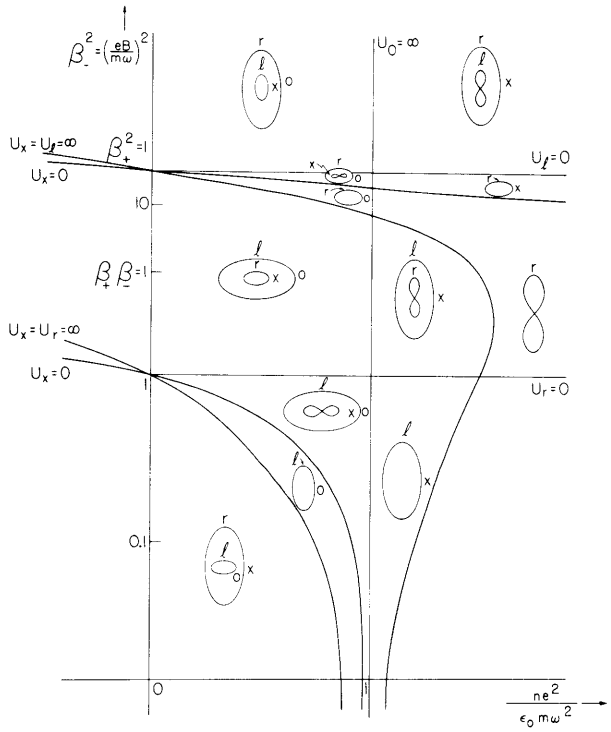

Fig. II-3. Wave normal surfaces of a plasma in a magnetic field, including the effects of ions.

complete wave surface; we use it in a different sense, and only for propagation normal to the magnetic field. (This is also Russian, but not Swedish, usage.) If we want a term for characterizing an entire wave surface, we should use "right-handed" and "left-handed," because this characterizes the direction of rotation of E around B for the entire surface. We must be cautious here, too, because the wave that we call "right-handed," rotates left-handed about the direction of propagation when it propagates along $-B$. A more satisfactory notation for an entire wave surface would be to denote it (rx), (ℓo), (x), and so forth.

We now wish to investigate the matter of which values of the parameters a, β_-, and θ give propagation ($n^2 > 0$), and which give attenuation ($n^2 < 0$). The boundaries of these regions are obviously the lines along which $n^2 = \infty$, $u = 0$, which we call "resonances," and those along which $n^2 = 0$, $u = \infty$, which we call "cutoffs."

The principal resonances are given by

$$K_r = \infty, \qquad \beta_- = 1, \qquad \text{Electron cyclotron resonance} \tag{16}$$

$$K_\ell = \infty, \qquad \beta_+ = 1, \qquad \text{Ion cyclotron resonance} \tag{17}$$

$$K_T = 0, \qquad a^2 = \frac{\left(1 - \beta_+^2\right)\left(1 - \beta_-^2\right)}{1 - \beta_+\beta_-}, \qquad \text{Plasma resonance} \tag{18}$$

The first two justify our definition of "resonance." The third is an extension of the conventional use of "plasma resonance" which applies when there is a magnetic field, but note that "plasma resonance" does not occur at the "plasma frequency" ω_p. For high frequencies ($\beta_+ \ll 1$) plasma resonance occurs at

$$\omega^2 = \omega_p^2 + \omega_{b-}^2 \tag{18a}$$

and is represented on a plot of β_-^2 against a^2 (Fig. II-1) by a diagonal straight line. In general, it is represented by a hyperbola

$$\omega^4 - \left(\omega_p^2 + \omega_{b-}^2 + \omega_{b+}^2\right)\omega^2 + \left(\omega_p^2 + \omega_{b+}\omega_{b-}\right)\omega_{b+}\omega_{b-} = 0 \tag{18b}$$

one branch of which goes through the points ($\omega_{b-} = 0$, $\omega = \omega_p$), and ($\omega_p = 0$, $\omega = \omega_{b-}$) and the other branch through ($\omega_p = 0$, $\omega = \omega_{b+}$) and ($\omega_p = \infty$, $\omega^2 = \omega_{b+}\omega_{b-}$). This last resonance, which occurs for large plasma densities ($n(M+m)c^2 \gg B \cdot H$), is sometimes called the "hybrid cyclotron resonance" but its relation to the cyclotron frequencies is accidental. At large plasma densities the electrons and ions must move together in the direction of the wave normal, otherwise charge separation would occur, but this is prevented by Coulomb forces; however, they may move parallel to the wave surface. At the particular frequency $\omega^2 = \omega_{b+}\omega_{b-}$ the equations of motion (7) show that the electron and ion

displacements in the direction of E are identical

$$\vec{\gamma}_{\pm} \cdot \vec{E} = eE^2/(m-M) \tag{19}$$

whereas at right angles to E the electrons have large displacements. The resonance occurs because Coulomb and electromagnetic forces independently make the electrons and ions move together along E.

There is no resonance for the ordinary wave but there are resonances along directions other than the principal directions. These are found by setting $n = \infty$ in Eq. 12:

$$\tan^2 \theta_{res} = -K_p/K_T \tag{20}$$

and occur whenever K_p and K_T have different signs. For a given plasma these directions occur on a cone whose axis is along B and whose angle θ_{res} depends on the frequency. In directions neare the resonant cone the phase volocity is slow and hence Čerenkov radiation is possible. Any electron in the plasma can have a "bow wave" which will be near the resonant cone (Fig. II-4).

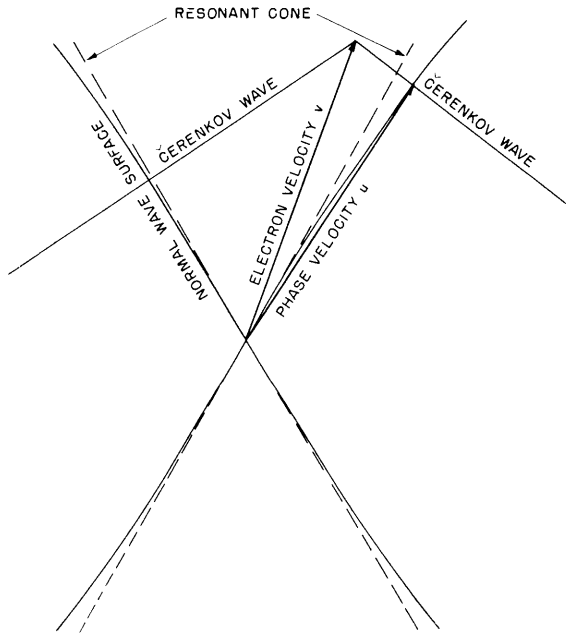

Fig. II-4. Čerenkov radiation near the resonant cone.

The resonant directions are also the directions in which plasma oscillations may occur, since it can be seen from Aström's expressions for the components of the electric vector that this vector becomes normal to the wave surface at any resonance.

The principal cutoffs are given by

$$\left.\begin{matrix} K_r = 0 \\ K_\ell = 0 \end{matrix}\right\} \quad a^4 = \left(1 - \beta_+^2\right)\left(1 - \beta_-^2\right), \qquad \text{Cyclotron cutoffs} \tag{21}$$

$$K_p = 0, \qquad a^2 = 1, \qquad \text{Plasma cutoff} \tag{22}$$

The two cyclotron cutoffs form a continuous curve which is a parabola on the $\beta^2 - a^2$ plot. The ordinary wave cuts off at the plasma frequency. There is no cutoff for the extraordinary wave. Neither are there cutoffs in other than the principal directions, because setting $n^2 = 0$ in Eq. 12 yields $\tan^2 \theta = -1$.

We are now ready to make a map of all possible wave surfaces by plotting β^2 against a^2 for all the principal resonances (Eqs. 16, 17, and 18) and cutoffs (Eqs. 21 and 22). Increasing the magnetic field would produce upward motion; increasing the plasma density would produce motion to the right; and decreasing the frequency for a given plasma and field would produce radial motion from the origin. Figure II-1 shows only the high-frequency range ($\beta_+ \ll 1$), in which only the electrons can follow the oscillations. As a resonance or cutoff line is crossed, one or two of the waves in the principal directions disappears, or reappears, and hence the shape of the wave surface changes radically. Within each of the eight areas in which the plane is divided we have plotted the corresponding normal wave surface with the direction of B parallel to the β-axis, calculated for some specific point in the area. The free-space light velocity is given by the dotted circles as a reference. There is one area in which there is no wave surface, as all waves are attenuated in this area. In the remaining seven areas there is propagation in some directions, but in only two of them do the two waves exist for all directions. Thus a plasma is largely opaque or largely transparent according to the way in which you look at it. Three of the areas have figure-eight, or figure-infinity, wave surfaces. These are the areas where K_p/K_T is negative and there is a resonant cone. The two points at ($\beta = 0$, $a = 1$) and ($a = 0$, $\beta_- = 1$) are extremely singular because both resonance and cutoff lines intersect there. Only the presence of a magnetic field removes the confusion about whether the plasma frequency ω_p is a resonance or a cutoff. The ordinary cutoff line at $a = 1$ is itself quite singular because on the low-density side of this cutoff the left-handed and ordinary waves are on the same wave surface, but on the high-density side it is the extraordinary wave that connects with the left-handed one. The transition is shown in Fig. II-2, in which four wave surfaces close to the plasma frequency are shown. At the plasma frequency the wave surfaces consist of a sphere close to the velocity of light

$$1/n^2 = 1/n_x^2 = 1 - \beta_+/\beta_-\left(\beta_+^2 - 1\right) \tag{23a}$$

but the polar points on this sphere are missing. They are replaced by two external points

$$1/n^2 = 1/n_\ell^2 = 1 + 1/\beta_- \tag{23b}$$

and two internal points (if they are real)

$$1/n^2 = 1/n_r^2 = 1 - 1/\beta_- \tag{23c}$$

On the left of $\alpha^2 = 1$ the sphere has dimples that connect with the internal points (or the origin). On the right of $\alpha^2 = 1$ the sphere has projections that connect with the external points.

As we approach the line $\alpha = 1$ from the right above cyclotron resonance, or from the left below cyclotron resonance, the resonance cone becomes very narrow. Thus although $\alpha = 1$ is not a resonance, it is always very close to a resonance for propagation very nearly along B.

The entire range of frequencies is shown in Fig. II-3, but logarithmic scales have had to be used and this obscures the simple shape of the resonance and cutoff lines. Even so, a small mass ratio of 4 had to be chosen so that the two small areas near ion cyclotron resonance would remain visible. There are now 13 areas with 12 distinct wave surfaces.

In the limit of low frequencies the figure-eight in the upper right-hand corner becomes two spheres tangent at the origin, and the elliptical figure becomes a sphere tangent externally to the two previous spheres. This sphere obeys Snell's law and is called the "ordinary wave" by Aström. We denote it (rx), and we have

$$\frac{1}{u_{rx}^2} = \frac{1}{c^2} + \frac{n(M+m)}{B \cdot H} \tag{24a}$$

where $(B \cdot H/n(M+m))^{1/2}$ is the Alfvén velocity. The other, termed "extraordinary wave" by Aström, is given by

$$u_\ell^2 = u_{rx}^2 \cos^2 \theta \tag{24b}$$

In regions where n^2 is negative the exponential (B) may be written

$$\exp (j\omega t - 2\pi \vec{n}^* \cdot \vec{r}/\lambda_o) \tag{25}$$

where λ_o is the free-space wavelength and $2\pi n^* = 2\pi jn$ is the attenuation per free-space wavelength. This attenuation is nowhere shown on our diagrams, but it is evident that n^{*2} rises linearly beyond any cutoff and jumps from zero to infinity at any resonance (Fig. II-5). Because we have removed all absorption mechanisms from our theory,

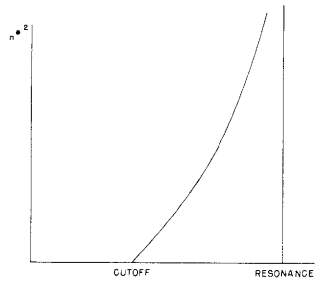

Fig. II-5. Variation of attenuation between cutoff and resonance.

a semi-infinite plasma will be perfectly transparent when $n^2 > 0$, and perfectly reflecting when $n^2 < 0$. A slab of plasma whose thickness is a finite number of free-space wavelengths will still be perfectly reflecting near a resonance, but near a cutoff considerable radiation may be transmitted.

W. P. Allis

References

1. A. G. Sitenko and K. N. Stepanov, J.E.T.P. (Soviet Physics) 31, 642 (1956).
2. J. E. Drummond, Phys. Rev. 110, 293 (1958).
3. T. H. Stix and R. W. Palladino, Phys. Fluids 1, 446 (1958).
4. I. B. Bernstein, Phys. Rev. 109, 10 (1959).
5. W. P. Allis, Motions of ions and electrons, Technical Report 299, Research Laboratory of Electronics, M.I.T., June 13, 1956, p. 17.
6. E. Aström, Arkiv Fysik 2, 443 (1950).
7. W. P. Allis, op. cit., p. 4.

B. MICROWAVE RADIATION FROM PLASMAS

In Quarterly Progress Report No. 54, page 4, we employed an extension of Nyquist's theorem to compute the microwave power P radiated from a plasma. For a plasma of arbitrary shape situated in a waveguide, the form of the theorem used was

$$P = kT\ A\ d\omega/2\pi \qquad (1)$$

where A is the fractional absorption suffered by a test wave that illuminates the plasma, T is the radiation temperature, and k is Boltzmann's constant. Here we shall verify this result for the case of a uniform plasma slab in a rectangular waveguide by considering in detail the individual emissions and their subsequent transport through the boundaries of the plasma slab.

Our procedure is to decompose the current associated with an electron's thermal motion between collisions in both space and time: its assumed square time pulse is Fourier-analyzed; its assumed delta-function spatial dependence is expanded in

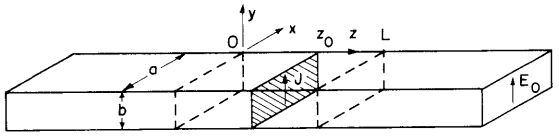

Fig. II-6. Schematic diagram of a current sheet in the waveguide.

current sheets appropriate to the waveguide modes. Only the current sheet exciting the dominant mode and the frequency components within the chosen interval will be retained.

For an electron at position (x_o, y_o, z_o) moving with y-component of velocity v_y, the spectrum density of the TE_{01} mode current sheet (see Fig. II-6) is

$$J(\omega) = J_y\sqrt{\frac{2}{\pi}} \sin\left(\frac{\pi y_o}{b}\right) \frac{\sin\left(\frac{\omega\tau}{z}\right)}{\omega} \tag{2}$$

where $J_y = ev_y/ab$ for $-\tau/2 < t < \tau/2$, and is zero elsewhere. The intensity spectrum density $I(\omega)$, defined as the power per frequency interval per unit area radiated into a 1-ohm load impedance is then found, after averaging over the distribution of collision times $\exp(-\tau\nu_c)$, with ν_c the collision frequency assumed constant.

$$I(\omega) = \frac{e^2v_y^2}{\pi(ab)^2} \frac{\nu_c}{\nu_c^2 + \omega^2} \sin^2\frac{\pi y_o}{b}\, d\omega \tag{3}$$

The contribution to the intensity radiated from an elemental slice dz about z_o of the plasma slab containing n electrons per unit volume, assumed to be radiating incoherently, is

$$I = dz \int_0^a dx_o \int_0^b dy_o\, n\mathscr{T} I(\omega) = \frac{ne^2\nu_c}{\nu_c^2 + \omega^2} \frac{v_y^2}{2\pi ab} \mathscr{T}\, d\omega\, dz \text{ watts/m}^2 \tag{4}$$

where $\mathscr{T}$ is the transfer impedance for a single radiative event, defined as the intensity, I, reaching the observer per unit intensity $I(\omega)$. We obtain the power dP flowing down the waveguide from the slice dz by integrating over the waveguide cross section; this yields $dP = (kT\, d\omega/2\pi)\sigma_r \mathscr{T}\, dz$ watts, after substituting $v_y^2 = v^2/3 = kT/m$ (with T, the electron temperature in degrees K), and $\sigma_r = ne^2\nu_c/\left[m\left(\nu_c^2 + \omega^2\right)\right]$ (with σ_r, the real part of the plasma conductivity $\sigma = \sigma_r + j\sigma_i$).

For a tenuous plasma $\mathscr{T} = Z\exp[-a(L - z_o)]$, where $Z = (\mu_o/\epsilon_o)^{1/2}(K - \lambda^2/4a^2)^{-1/2}$ is the waveguide impedance; K, the plasma dielectric coefficient assumed as close to unity; and a, the absorption coefficient of the plasma-filled waveguide. Integrating over all slices and

in the limit $aL \ll 1$, we obtain the total power from the slab

$$P = \frac{kT\, aL\, d\omega}{2\pi(1-\lambda^2/4a^2)^{1/2}} \quad \text{watts} \tag{5}$$

since $\sigma_r \approx a(\epsilon_o/\mu_o)^{1/2}$ when $\sigma_r/\sigma_i \ll 1$. It is seen that the power radiated increases with wavelength as cutoff ($\lambda = 2a$) is approached. Equation 5 is, of course, invalid near cutoff where the assumption that the plasma is tenuous does not hold.

In order to find $\mathscr{T}$ for a plasma of arbitrary opacity, it is necessary to solve the boundary-value problem of a current sheet in a uniform dielectric slab in a waveguide. The result of this calculation is

$$\mathscr{T} = \frac{1}{Z_o}\,\mathrm{Re}\left[\frac{\cos(\gamma z_o) + j(k/\gamma)\sin\gamma z_o}{2(k/\gamma)\cos(\gamma L) + j(1+(k/\gamma)^2)\sin(\gamma L)}\, Z\right]^2 \quad \text{ohms} \tag{6}$$

where Z_o is the empty waveguide impedance, γ is the (complex) propagation constant in the section of waveguide containing the plasma, and k is the (real) propagation constant in the empty waveguide. The power radiated by the slab then follows as $P = \int_0^L (kT\, d\omega/2\pi)\,\sigma_r\,\mathscr{T}\, dz$. This result reduces to Eq. 1.

Typical results of such a calculation are shown in Fig. II-7, together with two examples of the approximate geometrical-optics solutions (1) discussed previously. The normalized noise power P/P_m, defined as $P[kT(1-|\Gamma|)\,d\omega/2\pi]^{-1}$ versus $a\ell$, is plotted. Here, $\ell = L$ is the slab thickness, and $a = (4\pi/\lambda)\left[1+\sigma/j\omega\epsilon_o - (\lambda/2a)^2\right]^{1/2}$, with λ_c, the cutoff wavelength of the propagating mode. Curve b in Fig. II-7 is the geometrical-optics solution, and curves, c, d, and e show the results of the exact calculation. In contrast to the geometrical-optics solution, in which P/P_m is only a function of $a\ell$, the exact solution depends explicitly on the collision frequency ν_c and on the ratio of slab thickness to wavelength. In the examples shown, the free-space wavelength was 10 cm. When the plasma slab is sufficiently thick (Fig. II-7c), very good agreement is obtained with the approximate solution even though the collision frequency is small, and hence reflections from the plasma are large. The small undulations observed in Fig. II-7c are the result of internal reflections. If the slab thickness is decreased and the collision frequency increased simultaneously (Fig. II-7d) agreement with geometrical-optics solution is good. However, when the slab is very thin and the collision frequency small (Fig. II-7e), large oscillations occur, and then the exact solution bears no resemblence to the approximate one. In the limit of small absorption (not shown in Fig. II-7) the geometrical-optics and boundary-value computations reduce to the exact transparent limit (Eq. 5).

When the plasma is inhomogeneous and not in the form of a slab (which is the case in our experiments), only geometrical-optics solutions are available. We have chosen for our example a plasma cylinder of radius R with its axis perpendicular to the direction

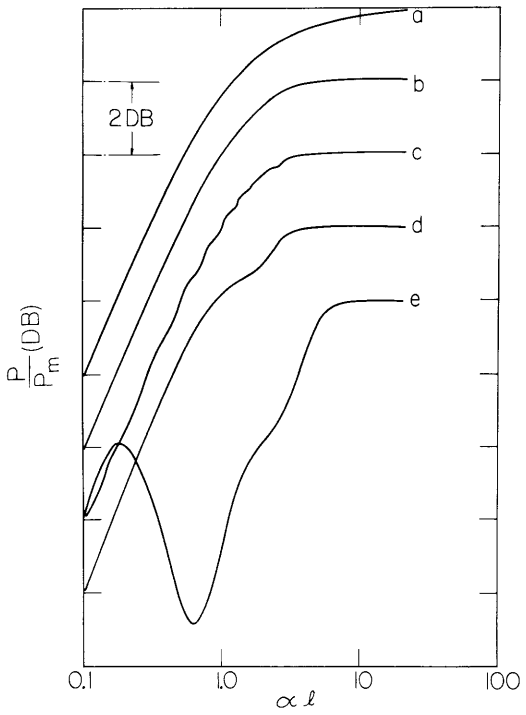

Fig. II-7. Radiation as a function of the attenuation coefficient of a plasma in a waveguide: (a) represents the geometrical-optics calculation for an inhomogeneous cylinder of radius R with $\ell = 0.678$ R; (b) geometrical-optics calculation for a slab of thickness ℓ; (c), (d), and (e), exact calculations for the slab. In (c), $\ell/\lambda_g = 7.2$, $\nu/\omega = 0.0292$; in (d), $\ell/\lambda_g = 1.0$, $\nu/\omega = 0.292$; in (e), $\ell/\lambda_g = 0.072$, $\nu/\omega = 0.0559$. (For clarity, curves are displaced vertically 2 db relative to each other.)

of propagation and to the electric field of the TE_{01} mode of a rectangular waveguide, and with a diameter equal to the narrow dimension of the waveguide. The absorption coefficient is assumed to vary in the radial direction r as the zero-order Bessel function and to vanish at r = R. (This implies that for low absorption coefficients, the electron density also varies as a Bessel function.) A plot of P/P_m versus $\alpha\ell$ is shown in Fig. II-7a. Here α denotes the absorption coefficient evaluated on the cylinder axis, and ℓ a characteristic length that, in this geometry, is given by $\ell = 0.678$ R.

J. L. Hirshfield, G. Bekefi

References

1. G. Bekefi and J. L. Hirshfield, Microwave noise radiation from plasmas, Quarterly Progress Report No. 53, Research Laboratory of Electronics, M.I.T., April 15, 1959, pp. 4-7.

2. S. J. Buchsbaum, Interaction of electromagnetic radiation with a high-density plasma, Ph.D. Thesis, Department of Physics, M.I.T., 1957.

(II. MICROWAVE GASEOUS DISCHARGES)

C. ELECTROMAGNETIC WAVE PROPAGATION IN A BOUNDED ANISOTROPIC PLASMA

Theoretical study of the physical properties of electron plasmas through their interaction with electromagnetic waves can easily be performed when boundary effects are minimized. For instance, the propagation properties of an infinite, homogeneous plasma are fairly well understood in terms of their interaction with plane electromagnetic waves. The practical problems involved in producing an infinite plasma and making measurements are, however, severe. Consequently, the experimental study of plasmas under controlled conditions is limited to bounded plasmas. Therefore the propagation properties of electromagnetic waves must be interpreted in terms of bounded structures containing plasmas.

The analytical formulation of this problem has been achieved for systems possessing cylindrical symmetry (dc magnetic field along the axis of symmetry) by following the procedure of Epstein (1). This formulation has been used for determining the various modes within a circular waveguide that contains a uniform, cylindrically symmetric plasma filament coaxial to the waveguide. When the plasma only slightly perturbs the propagation properties of the waveguide the effects may be interpreted either from this exact formulation or from the usual perturbation theory.

In a case of considerable practical interest – when the plasma does not act as a slight perturbation on the waveguide – the exact formulation, the interpretation of which requires numerical analysis, must be used. The eigenvalues (the propagation constant for a coaxial waveguide and the change in resonant frequency for a coaxial cavity) for the azimuthally symmetric modes are now being determined numerically by the Computation Center, M.I.T.

In the analysis, we assume that both the plasma and the bounding structure possess cylindrical symmetry with a uniform dc magnetic field directed along the axis of symmetry (z-axis). If we absorb the properties of the plasma in an effective dielectric tensor, then within the plasma the electromagnetic field must satisfy

$$\nabla \times \underline{H} = -\omega\epsilon_0 \overleftrightarrow{\underline{\epsilon'}} \cdot \underline{E}$$
$$\nabla \times \underline{E} = +i\omega\mu_0 \underline{H} \qquad (1)$$

where a time dependence of the form $\exp(-i\omega t)$ has been assumed. Here $\underline{E}$ and $\underline{H}$ are the electric and magnetic intensities, ω is the angular frequency of the wave, and ϵ_0, μ_0 are the characteristic constants of free space. MKS units will be used. The tensor dielectric constant, $\overleftrightarrow{\underline{\epsilon'}}$, has the elements

$$\underline{\overleftrightarrow{\epsilon}}' \equiv \begin{bmatrix} \epsilon_{11} & i\epsilon_{12} & 0 \\ -i\epsilon_{12} & \epsilon_{11} & 0 \\ 0 & 0 & \epsilon_{33} \end{bmatrix} \tag{2}$$

where the elements are functions of ω, the electron density, the magnitude of the dc magnetic field, the electron temperature, and so forth. The determination of these elements as a function of these parameters is of particular physical interest. Epstein's formulation is for a gyrotropic medium with the permittivity ϵ, a scalar, and the permeability μ, a tensor. The symmetry of Maxwell's equations allows us to introduce the transformation: $\underline{E} \rightarrow \underline{H}$, $\underline{H} \rightarrow -\underline{E}$, $\epsilon \rightarrow \mu = \mu_o$, and $\underline{\overleftrightarrow{\mu}} \rightarrow \epsilon_o \underline{\overleftrightarrow{\epsilon}}'$. The electromagnetic field within the plasma can be found from Epstein's formulation once this transfromation is performed.

Carrying out this transformation, we find that the electromagnetic field within the plasma is given by

$$\underline{E} = i \underline{\overleftrightarrow{S}}_E \cdot \nabla\left(\frac{\partial \Pi_j}{\partial z}\right) \qquad \underline{H} = \underline{\overleftrightarrow{S}}_H \cdot \nabla \Pi_j \qquad j = 1, 2 \tag{3}$$

in which we have used Epstein's notation. The elements of these two tensors are

$$\underline{\overleftrightarrow{S}}_E = \begin{bmatrix} a_j & ib & 0 \\ -ib & a_j & 0 \\ 0 & 0 & g_j \end{bmatrix} \qquad \underline{\overleftrightarrow{S}}_H = \left(\frac{\epsilon_o}{\mu_o}\right)^{1/2} \begin{bmatrix} i\sigma & \tau_j & 0 \\ -\tau_j & i\sigma & 0 \\ 0 & 0 & -i\sigma k_j^2/\gamma \end{bmatrix} \tag{4}$$

The scalar Π_j has the form $\phi(x, y) \exp i(\gamma z - \omega t)$ and must satisfy the two-dimensional Helmholtz equation

$$\frac{\partial^2 \Pi_j}{\partial x^2} + \frac{\partial^2 \Pi_j}{\partial y^2} + k_j^2 \Pi_j = 0 \tag{5}$$

where the k_j^2 are given by

$$\begin{Bmatrix} k_1^2 \\ k_2^2 \end{Bmatrix} = \left[\frac{\left(k_o^2 - M\gamma^2\right)(M + M_3) + K^2\gamma^2 \pm f}{2MM_3}\right] \tag{6}$$

with

$$f^2 = (M - M_3)^2 \left(k_o^2 - M\gamma^2\right)^2 + 2(M + M_3)\left(k_o^2 - M\gamma^2\right)K^2\gamma^2 + \left(K^2 + 4MM_3\right)K^2\gamma^4$$

and

$$k_o^2 = \omega^2 \mu_o \epsilon_o$$

The symbols in these expressions have the following definitions:

$$\left.\begin{aligned}
\sigma &\equiv K\gamma^2 \\
\tau_j &\equiv M\left(k_j^2 + \gamma^2\right) - k_o^2 \\
a_j &\equiv \left[M\tau_j - K^2\left(\gamma^2 + k_j^2\right)\right]/k_o \\
b &\equiv -K k_o \\
g_j &\equiv -M_3 k_j^2 \tau_j^2/k_o\gamma^2 \\
M &\equiv \epsilon_{11}/d \\
M_3 &\equiv 1/\epsilon_{33} \\
K &\equiv -\epsilon_{12}/d \\
d &\equiv \epsilon_{11}^2 - \epsilon_{12}^2
\end{aligned}\right\} \qquad (7)$$

From this formulation we see that the cylindrically symmetric plasma can support two partial fields. In the absence of boundaries (spatially infinite plasma) these fields are independent. However, in the presence of boundaries neither field is sufficient by itself to satisfy the boundary conditions, and so both fields must be used. The question of the completeness of this formulation has been touched upon by Epstein and will not be considered here.

We have applied this general formulism to the specific problem of the propagation of an electromagnetic wave within a circular waveguide of radius r_2 containing a uniform plasma "rod" of radius $r_1 < r_2$. In the region $0 \leq r \leq r_1$, the field is given by the superposition of both partial fields of expression 4. We consider as an example the azimuthally symmetric modes (quasi TE_{0m} and TM_{0m}). Consequently,

$$\Pi_j = A_j J_o(k_j r) \exp i(\gamma z - \omega t) \qquad j = 1, 2 \qquad (8)$$

Within the region exterior to the plasma the field (2) will be a superposition of the partial fields derivable from the Hertz potential involving J_o and N_o, which are Bessel functions of the first and second kind with coefficients $A_j (j=3-6)$. Using Eq. 8, we find that the field within the plasma ($0 \leq r \leq r_1$) is given by

$$E_r = -\gamma[A_1 k_1 a_1 J_o'(k_1 r) + A_2 k_2 a_2 J_o'(k_2 r)]$$

$$E_\phi = ib\gamma[A_1 k_1 J_o'(k_1 r) + A_2 k_2 J_o'(k_2 r)] \tag{9}$$

$$E_z = -i\gamma^2[A_1 g_1 J_o(k_1 r) + A_2 g_2 J_o(k_2 r)]$$

and

$$H_r = (\epsilon_o/\mu_o)^{1/2} [A_1 k_1 J_o'(k_1 r) + A_2 k_2 J_o'(k_2 r)]\, i\sigma$$

$$H_\phi = -(\epsilon_o/\mu_o)^{1/2} [A_1 \tau_1 k_1 J_o'(k_1 r) + A_2 k_2 \tau_2 J_o'(k_2 r)] \tag{10}$$

$$H_z = (\sigma/\gamma)(\epsilon_o/\mu_o)^{1/2} [A_1 k_1 J_o(k_1 r) + A_2 k_2 J_o(k_2 r)]$$

in which we have suppressed the common factor $\exp i(\gamma z - \omega t)$. The prime on J_o denotes the derivative with respect to its argument.

The boundary conditions are: at $r = r_1$, continuity of the tangential components of the electric and magnetic field; and at the waveguide wall, vanishing of the tangential component of the electric field. The imposition of the boundary conditions results in a set of six homogeneous equations for the coefficients A_j:

$$A_j B_{jk} = 0 \qquad k = 1, \ldots 6 \tag{11}$$

The necessary and sufficient condition for this set to have a nontrivial solution for the A_j is that

$$\det B_{jk} = 0 \tag{12}$$

The roots of this equation yield the propagation properties of the plasma-waveguide system. It is this determinant for which the roots will be found numerically. For reference, the nonzero elements of this determinant are given as follows:

$$B_{11} = J_1(\rho_1)$$

$$B_{12} = J_1(\rho_2)$$

$$B_{16} = (1 - x^2)^{1/2} J_o(\rho_2)$$

$$B_{21} = N_1(\rho_1)$$

$$B_{22} = N_1(\rho_2)$$

$$B_{26} = (1 - x^2)^{1/2} N_o(\rho_2)$$

$$B_{32} = -K(k_1/k_o)\, J_1(k_1 r_1)$$

$$B_{33} = M_3\left(k_1^2/k_o^2\right)\left[M\left(k_1^2/k_o^2 + x^2\right) - 1\right] J_o(k_1 r_1)$$

$$B_{34} = (k_1/k_o)\left[M\left(k_1^2/k_o^2 + x^2\right) - 1\right] J_1(k_1 r_1)$$

$$B_{36} = -K\left(k_1^2/k_o^2\right) J_o(k_1 r_1)$$

$$B_{43} = (1 - x^2)^{1/2}\, J_o(\rho_2)$$

$$B_{44} = J_1(\rho_2)$$

$$B_{45} = J_o(\rho_1)$$

$$B_{53} = (1 - x^2)^{1/2}\, N_o(\rho_2)$$

$$B_{54} = N_1(\rho_2)$$

$$B_{55} = N_o(\rho_1)$$

$$B_{62} = -K(k_2/k_o)\, J_1(k_2 r_1)$$

$$B_{63} = M_3\left(k_2^2/k_o^2\right)\left[M\left(k_2^2/k_o^2 + x^2\right) - 1\right] J_1(k_2 r_1)$$

$$B_{64} = (k_2/k_o)\left[M\left(k_2^2/k_o^2 + x^2\right) - 1\right] J_1(k_2 r_1)$$

$$B_{66} = -K\left(k_2^2/k_o^2\right) J_o(k_2 r_1)$$

Here $x = \gamma/k_o$, $\rho_1 = \gamma r_2(1/x^2 - 1)^{1/2}$, and $\rho_2 = \gamma r_1(1/x^2 - 1)^{1/2}$.

S. J. Buchsbaum, L. Mower

References

1. P. S. Epstein, Revs. Modern Phys. 28, 3 (1956).

2. J. A. Stratton, Electromagnetic Theory (McGraw-Hill Book Company, Inc., New York, 1941), p. 361.

D. MICROWAVE LOAD CURVES FOR PLASMA-LOADED CAVITIES

The production of a plasma in a microwave cavity is analyzed here as a circuit problem in which the plasma is a nonlinear load. In principle, the method is similar to that used for determining the operating state of a dc discharge from the intersection of the static load line and the volt-ampere characteristics of the discharge. The details, however, are more involved because of the interaction of the plasma on the resonance character of the microwave cavity. We hope that this analysis will eventually lead to an understanding of our experimental results and to the criteria for maximization of plasma density.

The basic microwave circuit is shown in Fig. II-8, together with the approximate equivalent circuit as viewed from a detuned short position in the line. The line impedance is referred to the cavity side of the coupling, where n^2 is the impedance ratio of the

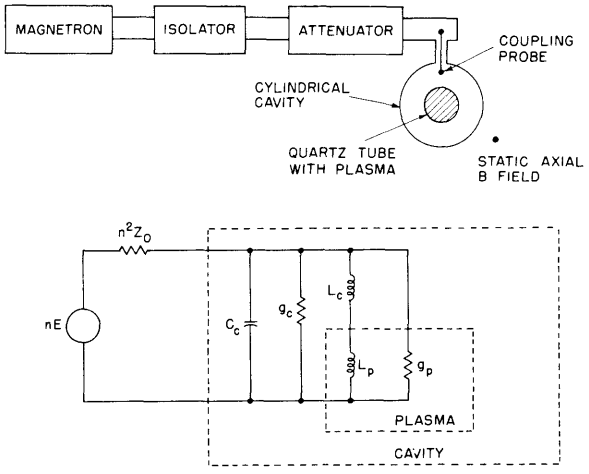

Fig. II-8. Microwave circuit, cavity, and plasma.

coupling probe. It has been assumed that the loss and reactance of the coupling probe are negligible. The equivalent capacitance, inductance, and conductance of the cavity are denoted C_c, L_c, and g_c, and the inductance and conductance of the plasma are denoted L_p and g_p. The parameters L_p and g_p can be obtained from theory by calculating the change in resonant frequency and Q of the cavity.

If it is assumed that the cavity contains a known plasma, then the expression for the power dissipated, P_{cp}, expressed as a fraction of the power available from the line into a matched load, P_a, is

$$\frac{P_{cp}}{P_a} = \frac{4\beta}{(1+\beta)^2} \frac{1}{1 + 4Q_L^2 \delta^2} \tag{1}$$

where

$$\beta = \frac{1}{n^2 Z_o (g_c + g_p)}, \qquad \text{total coupling coefficient}$$

$$\frac{1}{\beta} = g_c n^2 Z_o + g_p n^2 Z_o = \frac{1}{\beta_c} + \frac{1}{\beta_p}$$

$$Q_L = \frac{Q}{1+\beta}, \qquad \text{loaded Q}$$

$$\frac{1}{Q} = \omega(L_p + L_c)(g_c + g_p)$$

$$\delta = \frac{\omega - \omega_r}{\omega}, \qquad \text{frequency variable}$$

The amount of the power that is absorbed by the plasma, P_p, is given by

$$\frac{P_p}{P_a} = \frac{g_p}{g_p + g_c} \frac{P_{cp}}{P_a} = \frac{\beta}{\beta_p} \frac{P_{cp}}{P_a} = \frac{4\beta^2}{\beta_p (1+\beta)^2} = \frac{1}{1 + 4Q_L \delta^2} \tag{2}$$

This function is a normal resonance curve with an amplitude of $4\beta^2/\beta_p(1+\beta)^2$ and a bandwidth of ω/Q_L. The amplitude of the resonance curve is the largest fraction of the available power that can be absorbed by the plasma. If we express this fraction in terms of the initial cavity coupling β_c, and the plasma coupling β_p, we obtain

$$\left.\frac{P_p}{P_a}\right|_{\delta=0} = \frac{4\beta^2}{\beta_p(1+\beta)^2} = 4\left(\frac{\beta_c}{1+\beta_c}\right)^2 \frac{\beta_p}{\left(\beta_p + \frac{\beta_c}{1+\beta_c}\right)^2} \tag{3}$$

Since β_c is experimentally adjustable and β_p is inversely proportional to plasma density, a plot of Eq. 3 will show how to maximize the power input to the plasma. Figure II-9

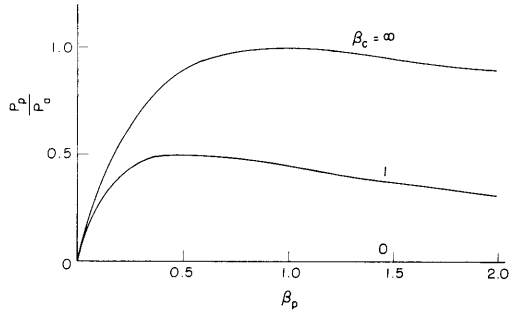

Fig. II-9. Absorbed plasma power versus plasma coupling coefficient.

shows the absorbed power as a function of β_p, with β_c as a parameter. This function has a maximum value of $\beta_c/(1 + \beta_c)$ when $\beta_p = \beta_c/(1 + \beta_c)$. From Fig. II-9 it is clear that the initial cavity coupling, β_c, ought to be highly overcoupled. The degree of overcoupling, however, need not be infinite, since the maximum absorbed power is 90 per cent for $\beta_c = 10$, and 99 per cent for $\beta_c = 100$. In most cases a 90 per cent efficiency would be sufficient.

Now that a criterion has been given for setting β_c, let us consider the use of microwave load curves to determine plasma density. For high-frequency discharges generated in resonant circuits, the variables of interest are power and frequency. Assume that a plasma characteristic is given which relates the power required as a function of plasma density for a given frequency, magnetic field, plasma and cavity geometry, and gas pressure. Since the change in resonant frequency of the cavity is a function of the plasma density, the plasma characteristic can more conveniently be plotted as the power required versus the change in resonant frequency. A typical experimentally determined plasma characteristic is shown in Fig. II-10. The abscissa is the fractional change of frequency

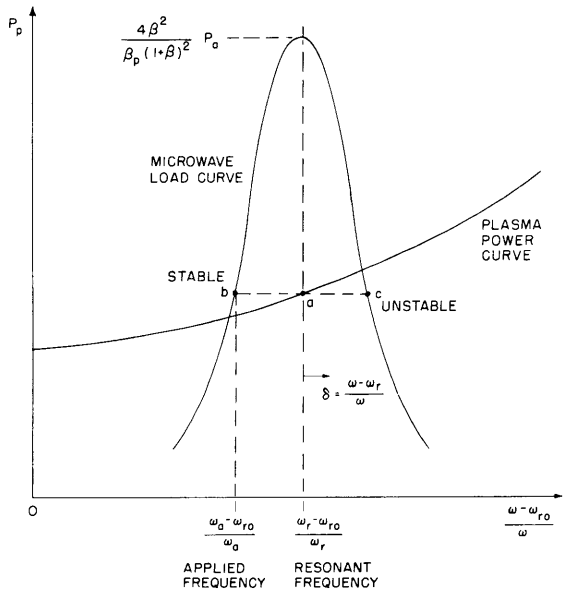

Fig. II-10. Microwave load curve construction.

from the empty resonant frequency of the cavity, $(\omega - \omega_{ro})/\omega$.

Next, a load curve must be drawn to determine the operating point. Here the details become involved because the load curve is a function of the plasma density and still it determines the plasma density. The height and width of the load curve, which is given by Eq. 2, changes with the plasma density. First, in a simple case, if the plasma density

is specified, say, at point a of Fig. II-10, then the corresponding load curve is centered above point a, and the necessary applied frequency to achieve this condition is determined from the intersection at point b. The more complicated procedure is to determine the density, and thus ω_r, if the applied frequency, ω_a, is given. In this case a trial and error procedure is followed to determine the load curve that satisfies the condition that the power into the plasma equals the power required by the plasma. The load curve in Fig. II-10 satisfies this condition. This construction is revealing in that it shows how the plasma density shifts the resonant frequency in order to receive the required amount of power. The excess power, of course, is reflected back into the waveguide. We also notice another frequency that intersects the load curve at point c and supplies the required power needs of the plasma. For the slopes of the curves indicated, point c is unstable because a departure from this point grows. It is conceivable, however, that if the slope of the plasma characteristic is very steep, point c could, in fact, be a stable operating point. A study of the stability of operating points b and c is continuing.

Besides the fact that the shape of the load curves is density-dependent, they can be shifted vertically by changing the power level with the attenuator in Fig. II-8. Since the actual Q of the load curve is much greater than the sketch shows, changing the available power P_a has a very small effect on the density. Changing the applied frequency, on the other hand, has a large effect on the density because the difference $\omega_a - \omega_r$ cannot change radically. If, by increasing the applied frequency, the density is increased to the level at which points b and a are coincident, the peak of the load curve is tangent to the plasma curve. A further increase in the applied frequency will extinguish the plasma. In fact, the plasma curve is deduced, in this manner, by measuring the incident power and coupling coefficient when the plasma is extinguished. Measurements are being made at the present time to determine the plasma curve as a function of density and magnetic field.

D. R. Whitehouse, J. D. Coccoli

E. MICROWAVE RADIATION FROM A PLASMA IN A MAGNETIC FIELD

Synchrotron radiation near the cyclotron frequency $\omega_b/2\pi = eB/2\pi m$, for individual charges undergoing a centripetal acceleration $v\omega_b$, with v the component of particle velocity normal to the magnetic field strength B, suggests that plasma radiation should be enhanced by this effect. Several recent calculations (1, 2, 3) emphasize that this effect is a strong mechanism for energy loss from a plasma. Here, it will be shown that this mechanism has been included automatically in the general approach that we have already applied to isotropic plasmas (4) with the advantage that the ordinary Bremsstrahlung of interparticle free-free transitions, as well as the effects of plasma opacity, are included.

We assume that detailed balancing applies, so that, again, the emission from a plasma is computed from its absorption coefficient through Kirchhoff's radiation law and applied to an anisotropic medium as discussed by Rytov (5) and Bunkin (6). The plasma absorption coefficients for the three possible waves propagating along a given direction, θ, with respect to the magnetic field have been discussed (7) extensively. We shall deal, in this report, with the low-temperature limit, wherein $v^2/c^2 \ll 1$, c representing light velocity, so that the plasma wave is neglected and zero-temperature values are used for the other two waves.

This approach is exemplified by calculating the radiation carried by the right-hand circularly polarized wave, that is, the wave propagating along the magnetic field, whose polarization rotates in the same sense as the electrons. For this wave, the absorption coefficient a is

$$a = \sqrt{2}\,\frac{\omega}{c}\left[(L^2 + M^2)^{1/2} - L\right]^{1/2} \qquad (1)$$

$$L = 1 - \frac{\omega_p^2(\omega - \omega_b)}{\omega\left[(\omega - \omega_b)^2 + \nu_c^2\right]} \qquad M = \frac{\omega_p^2 \nu_c}{\omega\left[(\omega - \omega_b)^2 + \nu_c^2\right]}$$

where $\omega_p = \left(ne^2/m\epsilon_o\right)^{1/2}$ is the plasma radian frequency, and ν_c is the collision frequency for momentum transfer. Strictly speaking, a term ν' should be added to the collision frequency to include radiation damping, $\nu' = \omega^2 e^2/6\pi\epsilon_o mc^3$. However ν' can be shown to be negligible compared with ν_c under usual plasma conditions.

When the plasma is sufficiently tenuous, that is, when $\omega_p^2/\omega_b \nu_c \ll 1$, Eq. 1 reduces to $a = \left(\omega_p^2 \nu_c/c\right)\left[(\omega - \omega_b)^2 + \nu_c^2\right]^{-1}$. Application of Kirchhoff's law in the Rayleigh-Jeans limit thus leads to the emission into a solid angle $d\Omega$ along B. We have

$$j(\omega)\,d\omega = \frac{\omega_p^2 \omega_b^2 \nu_c kT}{8\pi^3 c^2}\,\frac{d\omega}{(\omega - \omega_b)^2 + \nu^2}\,d\Omega \quad \text{watts/m}^3 \qquad (2)$$

This is seen to be a Lorentzian line shape that is typical for collision-broadened line spectra. We can show that Eq. 2 applies to emission into a solid angle in a direction θ with respect to B simply by multiplying $1/2(1 + \cos^2\theta)$. The total power is obtained by integrating over all solid angles and over all frequencies, which gives $J = ne^2(v\omega_b)^2/6\pi\epsilon_o c^3$ watts/m^3. We see that both the magnitude and the angular distribution of the radiation from a tenuous plasma as computed here agrees with what would be calculated as the energy loss from n incoherent electrons resulting from radiation damping (8). This result, in spite of our neglect of radiation damping in the absorption coefficient, is not surprising, however, because under our assumptions, the ordinary Bremsstrahlung has given way to a Bremsstrahlung arising mainly from charges

accelerated harmonically at a frequency $\omega_b/2\pi$.

Extension of Eq. 2 to include small thermal effects can be approximated by replacing ω_b with the Doppler-shift resonance frequency $\omega_b(1 - v/c)$, with $v/c \ll 1$. Here v represents the component of random velocity in the direction of the observer. The resultant must be averaged over the velocity distribution function. When Doppler and collision broadening occur simultaneously, tabulated functions give the resultant line shape (9). The relative importance of these two effects is seen by comparing v/c with ν_c/ω_b. For a magnetic field of 1070 gauss, v/c is equivalent to $2(T_v)^{1/2}$ gauss (T_v is the electron temperature in volts), and ν/ω_b is equivalent to p/8 gauss (p is the helium pressure in μ Hg).

With the use of the Dicke radiometer previously described (4), and of a horn in the far field of the plasma for receiving the radiation at 3000 mc, cyclotron radiation has been observed experimentally for waves propagating both along, and at right angles to, the B field. A typical resonance curve for $\theta = 0°$ is shown in Fig. II-11. This curve was obtained at a helium pressure of 20μ Hg so that its half-width of approximately 40 gauss is probably indicative of the inhomogeneity of the magnetic field because even the algebraic sum of the estimated Doppler plus collision "widths" is only approximately 13 gauss. Graphical integration under the line, with the electron-density value of 1.4×10^9 cm^{-3} deduced from mobility data used, gave an electron temperature of 32,000° K. This illustrates an application of Eq. 2.

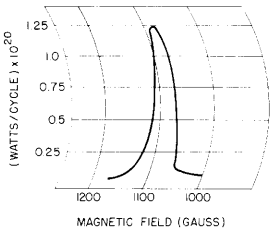

Fig. II-11. Observed cyclotron-resonance radiation from a transparant plasma.

When the plasma is not tenuous radiation must be computed by using the full form of the absorption coefficient (Eq. 1). The effects of opacity can be included in a typical way by using the approximate results for the radiation emitted normal to an infinite uniform slab of thickness L, where the power emitted has been shown (4) to be $P = kT\,d\omega(1-\Gamma)(1 - e^{-\alpha L})/\lambda^2$ watts/m^2, in which Γ is the reflection coefficient. We have previously discussed the limitations of this solution for isotropic plasmas. Figure II-12 shows the results of a calculation of $P/P_m = 1 - e^{-\alpha L}$ for $L = \lambda/(2\sqrt{2}\,\pi)$ and for various ratios of ν_c/ω. The curves for $\omega_p^2/\omega^2 = 0.01$ are generally representative of Eq. 2, and in each case half-widths are indicated. The effects of collisions and space charge are obvious. It is interesting to note how the curves approach those calculated in the limit $\nu_c \to 0$. In this limit the absorption coefficient computed from Eq. 1 does not represent true absorption at all; it merely describes the evanescence of a cutoff wave.

The frequency spectrum of radiation as described above is shown in Fig. II-13 in the

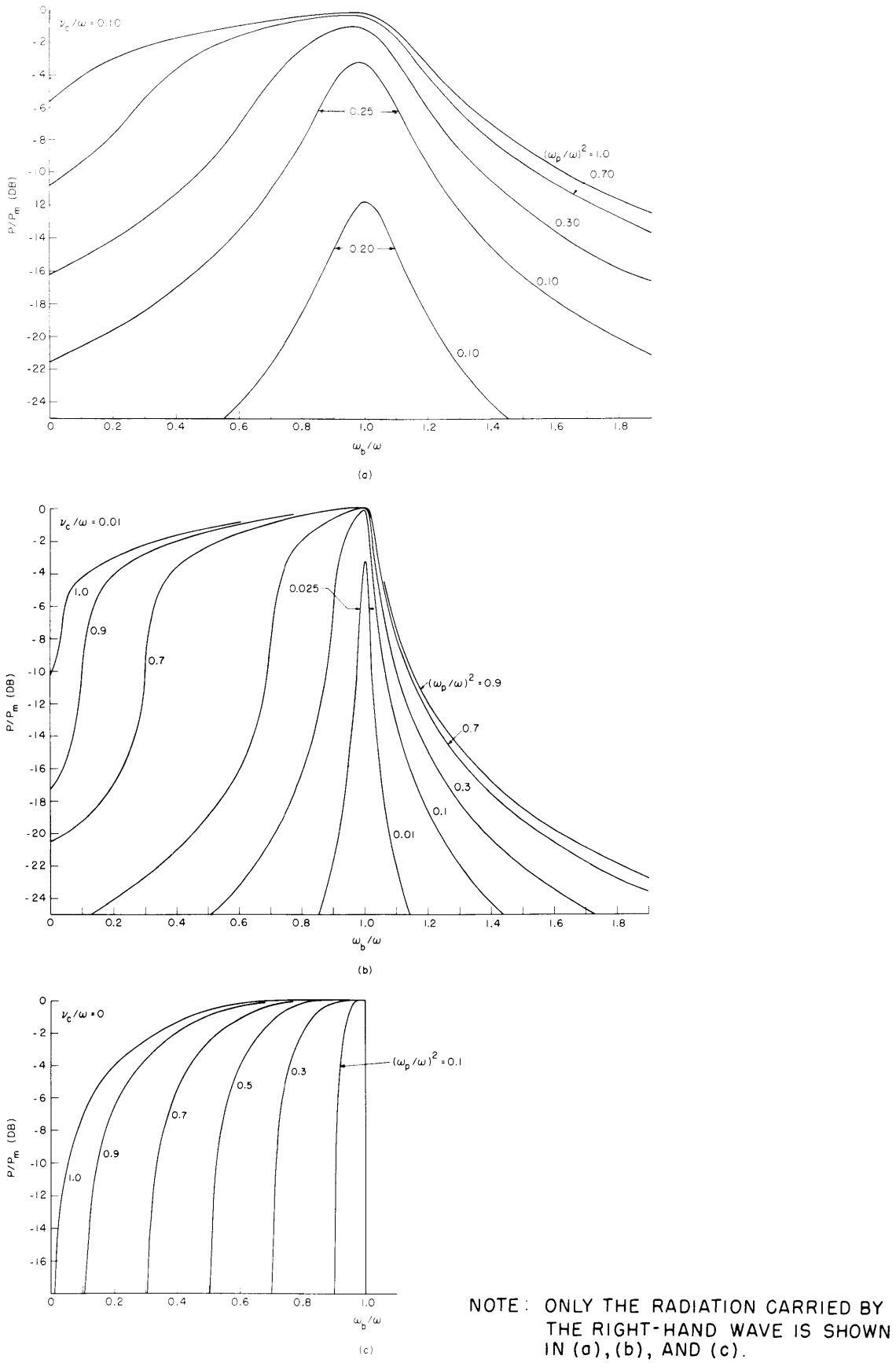

Fig. II-12. Calculated radiation from a plasma in a magnetic field.

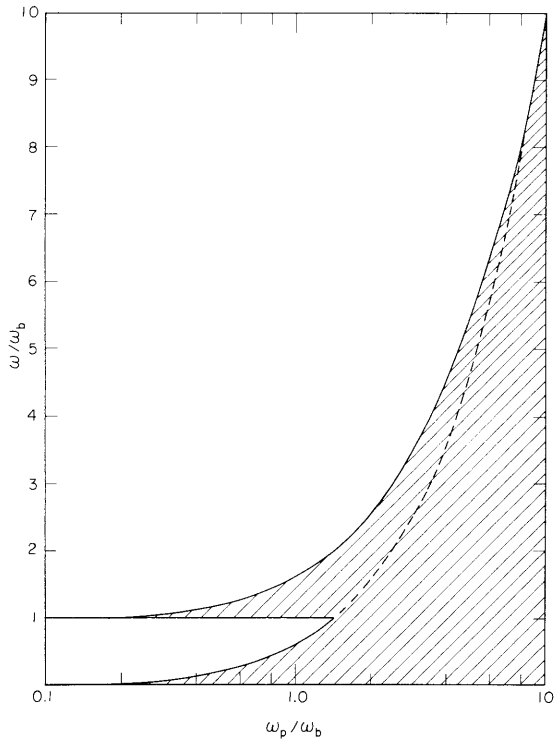

Fig. II-13. Frequency spectrum of black-body radiation.

limit of small ν_c/ω. In the crosshatched region, the plasma radiates essentially as a black body at temperature T; otherwise it is essentially transparent. The lower branch of the curve is the contribution from the left-hand wave. As ω_p/ω_b increases, the plasma radiates as a black body at frequencies up to $\omega = \omega_b$, so that here the effect of the magnetic field is completely obscured by the plasma space charge. This condition can be shown to be independant of θ.

J. L. Hirshfield

References

1. S. Hayakawa, N. Hokkyō, Y. Terashima, and T. Tsuneto, Cyclotron radiation from a magnetized plasma, a paper presented at the Second United Nations International Conference on the Peaceful Uses of Atomic Energy, Geneva, Switzerland, 1958.

2. B. A. Trubnikov and B. S. Kudryavtsev, Plasma radiation in magnetic field, a paper presented at the Second United Nations International Conference on the Peaceful Uses of Atomic Energy, Geneva, Switzerland, 1958.

3. D. B. Beard, Phys. Rev. Letters 2, p. 81 (1959); Incoherent microwave radiation from an ionized gas confined by a magnetic field, Technical Report 48394, Lockheed Missile and Space Division, Sunnyvale, California, 1959.

4. G. Bekefi and J. L. Hirshfield, Microwave noise radiation from plasmas, Quarterly Progress Report No. 52, Research Laboratory of Electronics, M.I.T., Jan. 15, 1959, pp. 6-12; No. 53, April 15, 1959, pp. 4-7.

5. S. M. Rytov, Theory of Electrical Fluctuations and Thermal Radiation (Izd-vo Akademiia Nauk S.S.S.R., Moscow, 1953).

6. F. V. Bunkin, J.E.T.P. (Soviet Physics) 5, 665 (1957).

7. L. Mower, Microwave properties of warm, anisotropic plasmas, Quarterly Progress Report No. 51, Research Laboratory of Electronics, M.I.T., Oct. 15, 1958, p. 21; W. P. Allis, Normal surfaces for electromagnetic waves in a plasma, Quarterly Progress Report No. 54, Research Laboratory of Electronics, M.I.T., July 15, 1959, p. 5.

8. H. Rosner, Motions and radiation of a point charge in a uniform and constant external magnetic field, Report AFSWC-TR-58-47, Republic Aviation Corporation, Farmingdale, L.I., New York, 15 Nov. 1958.

9. L. H. Aller, Astrophysics – The Atmospheres of the Sun and Stars (The Ronald Press Company, New York, 1953), pp. 251-256.

F. A LIMITATION OF RF CONFINEMENT

The time-averaged force on a charged particle in a high-frequency field is given by

$$\bar{f} = -\frac{1}{4}\frac{q^2}{m\omega^2}\nabla E^2 \qquad (1)$$

Equation 1 is valid when collisions are negligible and there is no external dc magnetic field. The force given by (1) acts to move particles toward weaker field strength regions.

A particular confining field pattern in a cylindrical cavity that has been previously considered is the TM_{011} mode. The electric field, in the transverse direction, of this mode is in the radial direction and increases with distance from the axis. According to Eq. 1 charged particles have a force tending to repel them toward the axis. The question arises though whether this type of field pattern will confine a low-density plasma. Since single particles are confined, the effect of the plasma on the rf electric field must be considered.

If one plots the unperturbed radial electric field of the TM_{011} mode, it appears as shown in Fig. II-14 (for points near the axis). On the other hand, if the plasma is confined by the electric field, it will have a density distribution somewhat like that shown

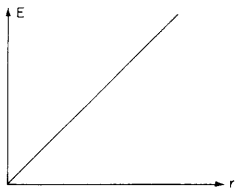

Fig. II-14. Unperturbed electric field.

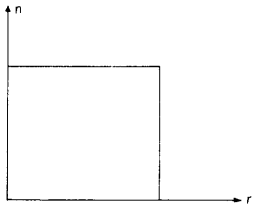

Fig. II-15. Confined plasma density.

in Fig. II-15. The electric field must satisfy the boundary condition of continuous ϵE, since the plasma has an effective dielectric constant ϵ_p. We have

$$\epsilon_p = \epsilon_o \left(1 - \frac{\omega_p^2}{\omega^2}\right) \tag{2}$$

and thus

$$\epsilon_p E_p = \epsilon_o E_o \tag{3}$$

For low-density plasmas ($\omega_p < \omega$), $\epsilon_p < \epsilon_o$, and thus, in order to satisfy Eq. 3, $E_p > E_o$. The resultant field pattern then is as shown in Fig. II-16.

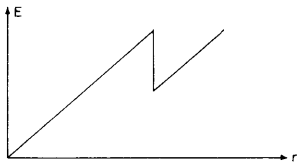

Fig. II-16. Field pattern of low-density plasma in the TM_{011} mode.

Since the electric field of the confining electric field decreases at the edge of the "confined" plasma, every particle that arrives at the plasma boundary will experience a force outward. This is an unstable situation and the plasma, in reality, cannot be confined, because the boundary will move outward. Thus, low-density plasmas ($\omega_p < \omega$) cannot be confined by electric fields that are perpendicular to the plasma boundary. The solution to this restriction is, of course, to use electric-field patterns that are entirely tangential to the plasma boundary or to obtain plasma densities high enough so that $\omega_p^2 > 2\omega^2$.

R. B. Hall

G. PLASMA DIAMAGNETISM

In an effort to verify the theory of plasma diamagnetism proposed by W. P. Allis (1), two experiments have been performed. These experiments were performed with long cylindrical dc discharges, and hence involved axial electric fields and currents with resulting azimuthal magnetic fields. However, over the range of our experiments these effects were theoretically shown to be negligible.

With the use of the small-signal approximation, the magnetic field depression is

$$\delta B = \frac{-\mu_+ \mu_- B_o}{1 + \mu_+ \mu_- B_o^2} \mu_o ne(T^+ + T^-) \tag{1}$$

where μ_+ is the ion mobility, μ_-, the electron mobility, μ_o, the free-space specific permeability, T, the temperature (electron-volts), B_o, the externally applied magnetic field, n, the electron density, and e, the electronic charge.

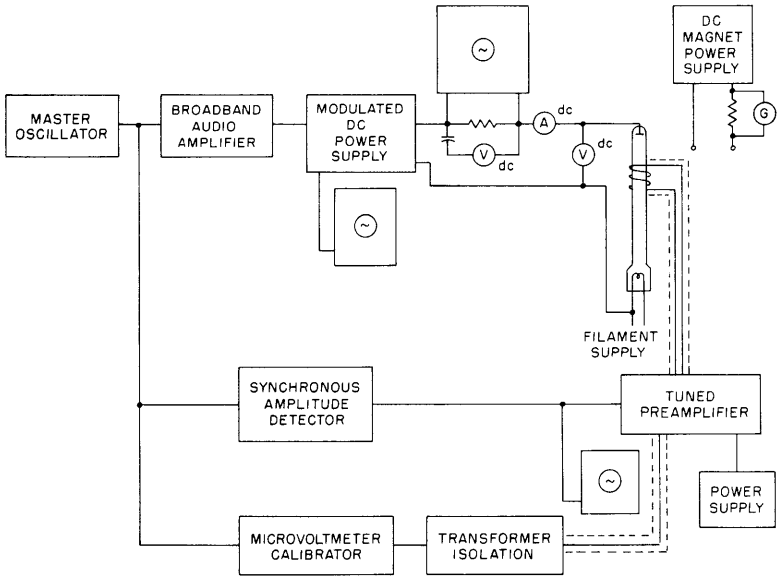

Fig. II-17. CW diamagnetic measurement system.

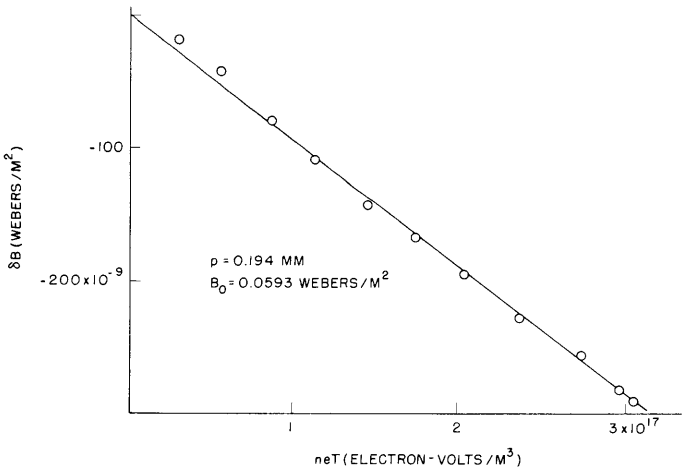

Fig. II-18. Plasma diamagnetism of helium.

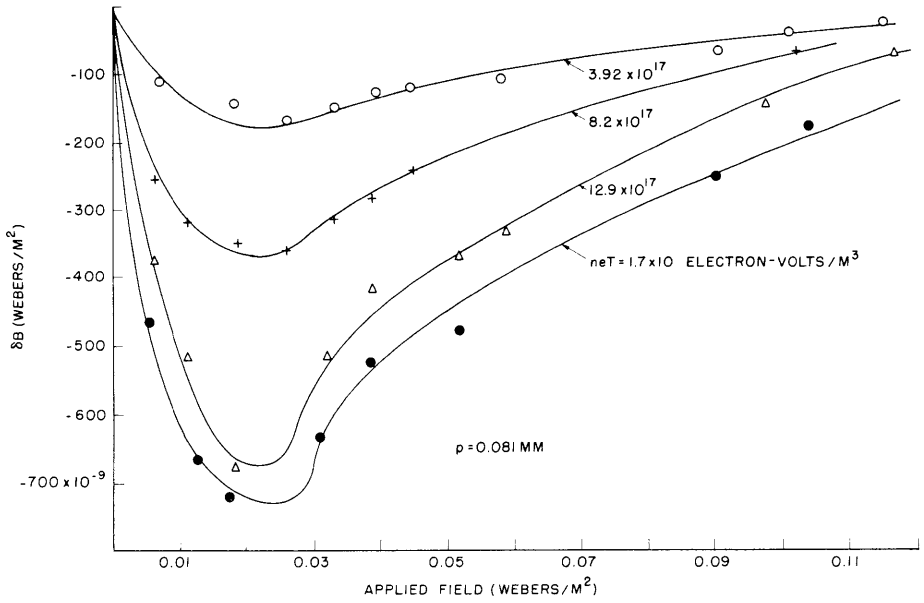

Fig. II-19. Plasma diamagnetism of helium.

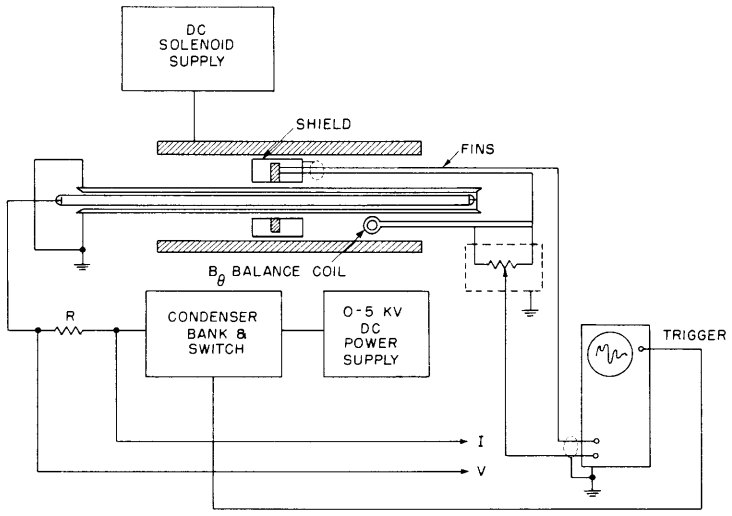

Fig. II-20. Pulsed diamagnetic measurement system.

Because of the experimental difficulties involved in varying the magnetic field, we decided to vary the plasma density. In order to measure the change in magnetic field, a pickup coil was used in the radial plane. In the first experiment (Fig. II-17), the density was varied sinusoidally by modulating the applied potential across the discharge. The output of the pickup coil was detected synchronously by using the modulation source as a reference. Data were obtained for the diamagnetic depression as a function of neT

and the applied magnetic field. Representative samples of the data are shown in Figs. II-18 and II-19.

Many difficulties were encountered in determining the density distribution. Longitudinal striations formed at low pressures (< 200 microns). At these low pressures, a large depression and an equally large augmentation of the applied magnetic field were observed. There seems to be no obvious explanation for this anomaly which occurs only over a very narrow region of the applied field. This anomaly has not been included in Fig. II-19.

In the pulsed experiment (Fig. II-20), a condenser bank was discharged through a cold-cathode tube to produce the plasma, and oscillograms were made of the output of the pickup coil. The B_o coil was used to cancel the spurious pickup of the axial field. The data obtained qualitatively follow the results of the first experiment described.

If the validity of Eq. 1 is assumed, the computed mobilities do not agree with the accepted values. Further experimentation must be carried out to satisfactorily establish the theory.

R. Glosser, G. Huguenin, P. Johansen

References

1. W. P. Allis and S. J. Buchsbaum, Diamagnetism of a long cylindrical plasma, Quarterly Progress Report, Research Laboratory of Electronics, M.I.T., July 15, 1958, pp. 5-10.